JOURNAL OF CATALYSIS 136, 320–333 (1992)

Embedded Atom Calculations of the Equilibrium Shape of Small Platinum Clusters

A. SACHDEV,* R. I. MASEL,*,[1] AND J. B. ADAMS†

*Department of Chemical Engineering, University of Illinois, 1209 W. California St., Urbana, Illinois 61801; and †Department of Materials Science, University of Illinois, 105 S. Goodwin St., Urbana, Illinois 61801

Received October 10, 1991; revised February 13, 1992

The embedded atom method was used to examine the shapes and stability of a series of platinum clusters with 5–60 atoms. The calculations suggest that the polyhedral structures seen in previous calculations are not stable. While the magic-number icosahedrons, cubo-octahedrons, tetrahedrons, and octahedrons retain their shape at 0 K, they spontaneously reconstruct upon annealing to 300 K. The nonmagic-number truncated icosahedrons, cubo-octahedrons, tetrahedrons, and octahedrons spontaneously reconstruct even at 0 K. A 147-atom icosahedron was also found to reconstruct to a lower energy structure upon annealing to 500 K. In contrast, there are a series of lower energy structures which are reasonably stable at 100–300 K. These lower energy structures are highly disordered and show surface structures which are not present in bulk platinum. At this point the calculations have not yet considered the effects of the support. However, these results suggest that small platinum clusters may be much more disordered than previous calculations suggest.

I. INTRODUCTION

The shape and microstructure of small metal particles in a catalyst can have a major influence on the catalyst's activity and selectivity. Most of the ideal models of the shapes of particles in catalysts come from work in the 1960s. Hoare and co-workers (*1–4*) calculated the shapes of argon clusters at 10–60 atoms, and found that perfect icosahedral and cubo-octahedral geometries were favored in argon clusters of these sizes. Hoare's calculations have been verified both experimentally (*5*) and computationally (*6–10*) for solid argon and they have been used to make predictions about catalysts. However, it is unclear to what extent these calculations apply to metal particles in catalysts. For example, previous workers (*11–14*) have found that small fcc metal particles supported on various substrates do not show the very regular particle shapes and structures predicted by Hoare's calculations. Instead, the particles have irregular shapes. Features such as twinning boundaries and stacking faults are quite prevalent. Investigators say they observe icosahedrons. However, the "icosahedral" particles are always multiple twinned. Larger particles tend to have rounded shapes under clean conditions (*15*). Simple metals show non-icosahedral shapes even in the gas phase (*34*). Therefore, there is reason to suspect that these older calculations using argon potentials do not apply to platinum group metals.

In this paper we have used a modern calculational procedure called the "Embedded Atom Method" (EAM) to determine the equilibrium shapes of small platinum clusters. The EAM technique was developed by Daw and Baskes (*16*) as a way of modeling the interaction of a metal atom with its surroundings. Basically, one divides the interaction of an atom with its neighbors into two terms, a two-body repulsion due to overlap at the atom with adjacent atomic cores and a multibody attraction due to overlap of the

[1] To whom correspondence should be addressed.

0021-9517/92 $5.00

atom with the conduction and d-bond electrons from its neighbors, and uses semiempirical potentials for both terms. EAM has been used to successfully predict the structure of small platinum clusters (3–6 atoms) adsorbed on Pt(100) field emitting tips (*17, 18*). It also has been used to accurately predict the stable surface reconstructions of the Pt(110) (*19, 20*), Pt(001) (*18*), and Pt(210) surfaces (*21*). Generally, the predicted structures show good agreement with experiment surface energies. The calculated surface energies are less accurate, but the variation in the surface energy with surface structure does show the correct trends. The EAM has also been used successfully to model the shapes of copper and nickel clusters (*22, 23*). Therefore, there is reason to suspect that EAM may also give good structural predictions for platinum clusters. In this paper, we use EAM to calculate the equilibrium structure and shape of platinum clusters containing 5–60 atoms.

We did several different kinds of calculations. The first was a stability analysis where we started with a fixed shape (e.g., an icosahedron) and did a conjugate gradient (CG) minimization (*24*) to calculate a relaxed shape. Such computations were conducted for platinum clusters ranging in size from $N = 5$ to $N = 60$ atoms. Calculations for the 147-atom magic-number icosahedral cluster were also performed. In addition, growth sequences were initiated to study some of the non-magic-number size clusters. Finally we did a series of simulated annealing studies to assess the stability of our clusters, and to search for lower energy structures.

II. METHODS

All of the calculations in this paper were done using a slightly modified version of the EAM code provided by Foiles, Daw, and Baskes (*16*). The code divides E_i, the interaction of an atom with its neighbors, into an embedding energy $F_i,(\rho_i)$, and an electrostatic pair interaction term, $\phi_{ij}(R_{ij})$:

$$E_i = F_i(\rho_i) + \frac{1}{2}\sum_{i,j}\phi_{ij}(R_{ij}).$$

The embedding energy is defined as the energy required to introduce atom i into the local electron density, ρ_i, created by the presence of the neighboring atoms. The pairwise repulsion term, ϕ_{ij}, is characterized by a Coulombic $1/r$ interaction, where the effective charges of the two atoms are functions of the interatomic separation. Foiles, Baskes, and Daw (*25*) have already created good semiempirical EAM functions for platinum and we used their functions without change.

The cluster symmetries examined in this study were the icosahedron, cubo-octahedron, octahedron and the tetrahedron (see Fig. 1). The make-up of these clusters can be most conveniently visualized in terms of a shell or layer type construction. For example, the 55-atom icosahedron has 12 atoms surrounding a central atom in the first shell and 42 atomic positions in the second shell. The so-called magic number represents the total number of atoms in a cluster when the shell sites are completely filled. In this way, the icosahedron magic numbers turn out to be 13, 55, and 147 for the first, second, and third shell, respectively. The cubo-octahedron also has the same magic numbers as that of the icosahedron, but its structure is characterized by the presence of square (100) and triangular (111) facets while the icosahedron has only (111) facets. These facets on the icosahedron represent the surfaces of the tetrahedral units which comprise the cluster. Similarly, the first two tetrahedron magic-number clusters are composed of 5 and 57 atoms, whereas the complete octahedral symmetry is obtained with 7 and 45 atoms. The octahedron and cubo-octohedrons are fcc structures, while the tetrahedron and icosahedron have symmetry elements which are not found in fcc materials.

III. RESULTS

Our first calculation was to start with a cluster of known geometry, e.g., an icosahedron with bulk lattice parameters, and do a conjugate gradient minimization of the clus-

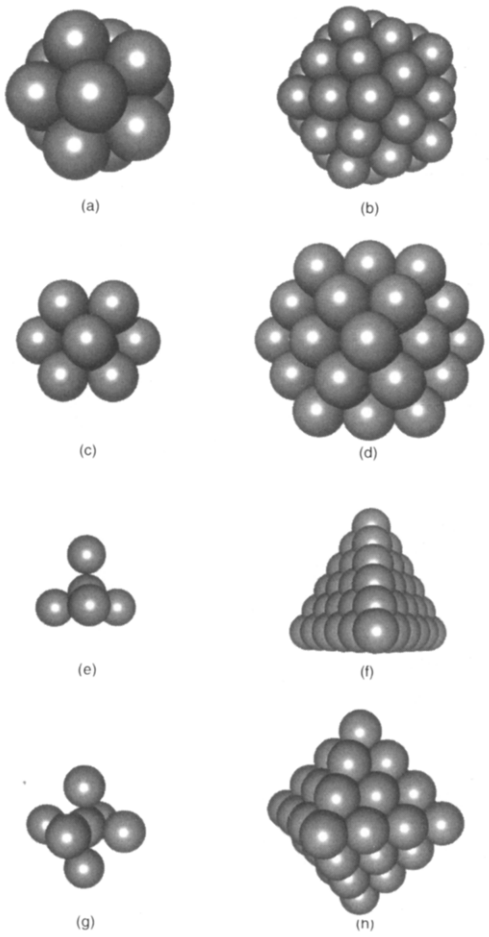

FIG. 1. The crystal shapes of the magic-number polyhedra: (a) $N = 13$ icosahedron (b) $N = 55$ icosahedron, (c) $N = 13$ cubo-octahedron, (d) N = 55 cubo-octahedron, (e) 5-atom tetrahedron, (f) 57-atom tetrahedron (g) 7-atom octahedron, and (h) 45-atom octahedron.

ter shape. One might have thought that the particles would retain their basic shape, upon energy minimization. However, we quickly discovered that with the exception of the 13- and 55-atom (i.e., magic-number) icosahedra, all of the other polyhedral particle shapes would spontaneously reconstruct into lower energy structures with twins and/or defects upon energy minimization. For example, Fig. 2 is an illustration of the reconstructions seen with 14- and 18-atom truncated icosahedra. We started with a minimized 13-atom icosahedron, added atoms at their icosahedral positions in the second shell, and then did a minimization. We find that with 14 atoms, the extra atom moves into the first shell, and all of the other first-shell atoms move to accommodate it. The result is a compact structure. However, the five-fold symmetry of the 13-atom icosahedron core is lost. Even larger distortions are seen with 18 atoms. Hence, we concluded that neither the 14- nor the 18-atom truncated icosahedra are stable.

This was a general trend; whenever we started with a nonmagic-number cluster it relaxed into a far more compact structure. Clusters relaxed from truncated-icosahedron structures have the unfavorable vertex site eliminated and instead now have a more equitable distribution of coordination numbers. We were able to create metastable 13- and 55-atom cubo-octahedra, 5- and 57-atom tetrahedra, and 7- and 45-atom octahedra by first minimizing the energy of the cluster with respect to the lattice dimension, relaxing each shell of atoms independently, and then doing a final re-relaxation allowing all of the atoms to move. The magic-number

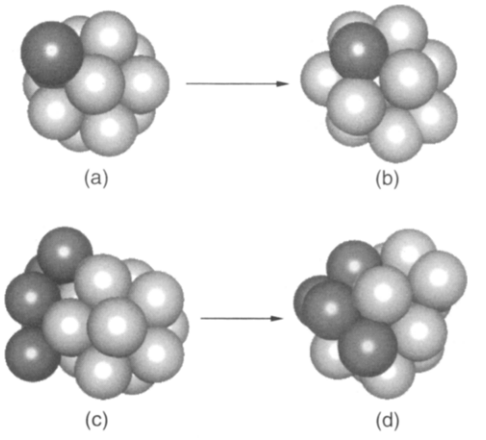

FIG. 2. An illustration of the shape changes which occur during the conjugate-gradient minimization of nonmagic-number truncated-icosahedral structures. (a) Initial 14-atom truncated-icosahedron, (b) relaxed 14-atom structure, (c) initial18-atom truncated-icosahedron, (d) relaxed 18-atom structure.

cubo-octahedra created in this way were found to be metastable in that they remain in the same symmetry as the starting cluster after "re-relaxation." The 45-atom octahedron and 57-atom tetrahedron distorted but only slightly. On the other hand, all of the nonmagic-number clusters relaxed into structures which no longer resembled the starting polyhedral symmetries. Consequently, it can be concluded that, in platinum the polyhedral shapes are not stable, except at the magic numbers.

III.1. Growth Sequences

Still, we were interested in finding a way to assess the energies of the nonmagic-number truncated-polyhedral structures, and so we adopted a rather ad-hoc procedure. We started with a closed shell core of atoms and added atoms one at a time at the correct second shell polyhedral positions to produce a growth sequence. For example, we started with a minimized 13-atom icosahedron and added a single atom as shown in Fig. 2a. We then calculated the energy of the cluster. A second atom was added with the criterion that its atomic position would minimize the total energy of the cluster. This additional atomic position was chosen such that it would be appropriate for an icosahedron. We emphasize that these are not minimized structures; if we do an energy minimization the cluster spontaneously reconstructs into an even lower energetic state such that it would no longer resemble the initial cluster symmetry.

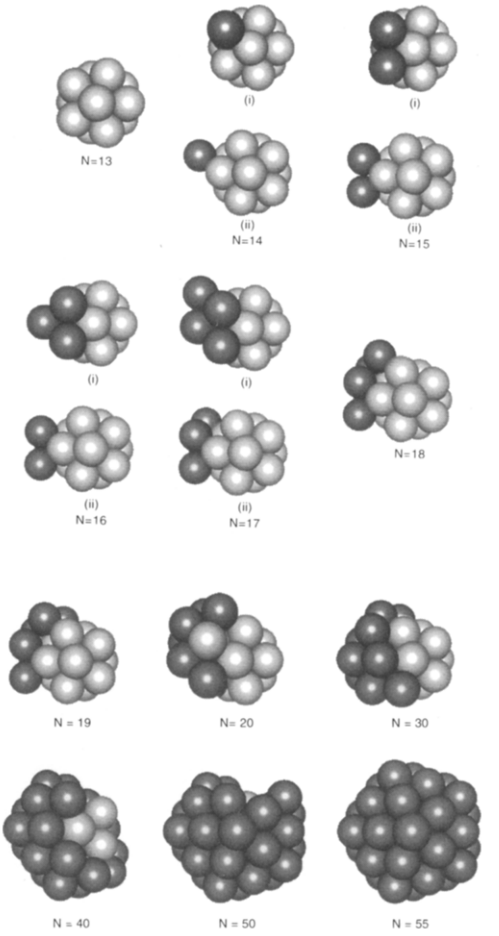

FIG. 3. A growth sequence calculated by starting with a 13-atom relaxed icosahedron and adding atoms in the best icosahedral positions. Note that none of these clusters are stable. If we do a conjugate gradient minimization the clusters will relax as shown in Fig. 2.

Figure 3 shows the growth sequence we have obtained, for the icosahedral structure. We start with the 13-atom cluster shown in Fig. 3 and add an atom. Referring back to Fig. 1, note that the atom can go into either an edge site or a vertex site. However, we find that energetically, it is more favorable for the atom to go into the edge site than into the vertex site. The atom has more nearest neighbors at the edge site. As a result, the embedding energy is larger at the edge site than the vertex site. The 15th atom and 16th atom also go into an edge site. When there is a 14th atom on the edge site, it is slightly more favorable for the 15th atom to occupy an adjacent edge site than to occupy an edge site far away from the 14th atom. As a result, the 15th atom goes on an edge site which is in close proximity to the 14th atom. The 16th atom also goes on an edge site to fill out the edges of a face, then the 17th atom goes on the vertex between the 14th, 15th, and 16th atom. The 18th atom goes to an edge site adjacent to the 14th, 15th, and 16th atom, and the sequence repeats. This pat-

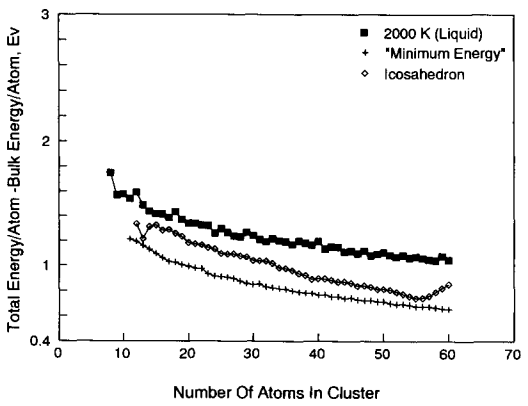

FIG. 4. The energy per atom minus the bulk energy per unit calculated for a growth of an icosahedral cluster with a frozen 13-atom core. Curves for the minimum energy clusters, and platinum clusters at 2000 K are included for comparison.

tern of filling of three or four edge positions followed by a single vertex atom is continued until the second shell is occupied. The last two positions in the growth sequence, or the least stable, happen to be vertex atoms.

Figure 4 shows the energy/atom minus the bulk energy/unit atom calculated for the clusters in the growth sequence in Fig. 3. The figure also included plots of the energy of a set of fully relaxed "minimum-energy clusters," see Section III.2, and the energies calculated from Monte Carlo simulations of liquid clusters at 2000 K.

At 13 atoms the icosahedron is fairly stable, but if we add a 14th atom in the icosahedral position the cluster energy jumps markedly. Referring back to Fig. 3, note that when we force the 14th atom into an icosahedral position, the 14th atom has only two nearest neighbors. By comparison, the atom would have three nearest neighbors if it were at a three-fold hollow, and nine nearest neighbors in the fully relaxed position shown in Fig. 2b. Energetically it is rather unfavorable to add the 14th atom in an icosahedral position. As a result, the energy at the cluster jumps when we force the atom to go into the icosahedral position. This feature in the growth sequence is not limited to our EAM calculations but has also been observed in calculations using the older argon pair potentials (*26*).

The energy/atom goes up with the 15th atom too, but then the energy/atom goes down with the 16th atom and the 17th atom. The 18th and 19th atom decrease the energy slightly. However, the 20th atom has a larger effect, since 20 atoms fill a complete face in the final icosahedron. This trend continues with increasing size. However, even with 55 atoms, the cluster still has an energy of 0.6 eV above the bulk.

We have also done growth calculations for cubo-octahedral, octahedral, and tetragonal clusters. Figure 5 compares the energy/unit atom calculated for these other cluster shapes to those for icosahedra. Note that of the four different cluster symmetries examined only the icosahedron and the cubo-octahedron are energetically competitive. The tetrahedron and the octahedron are especially unstable at the nonmagic-number sizes. With small clusters the total energy of a cluster with tetrahedral coordinates is even higher than the corresponding liquid cluster at 2000 K. The cluster sizes in the middle of the growth sequence are similar in energy and shape irrespective of the initial polyhedra. Physically, however, the various

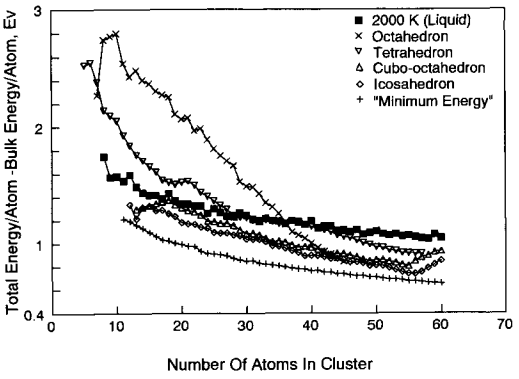

FIG. 5. The energy per atom minus the bulk energy per atom for the growth of (◇) truncated icosahedra, (△) truncated cubo-octahedra, (▽) truncated tetrahedra, (×) truncated octahedra, (■) platinum clusters at 2000 K, and (+), the "minimum energy" clusters.

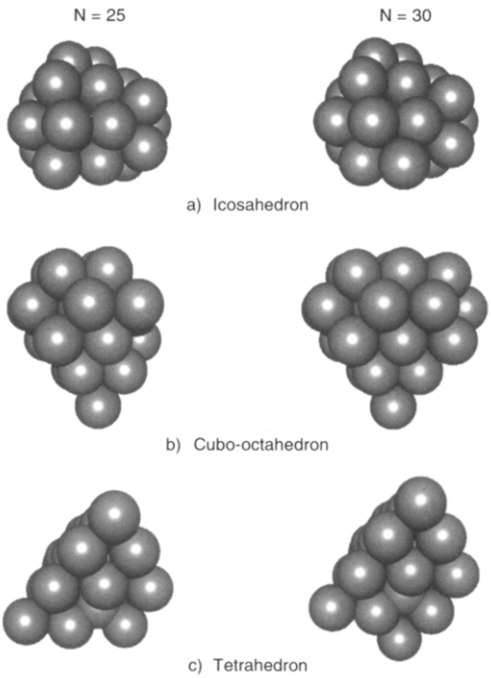

FIG. 6. A comparison of the structure of $N = 25$ and $N = 30$ truncated icosahedra, truncated cubo-octahedra, and truncated tetrahedra.

structures are not that much different in the middle of the growth sequence, see Fig. 6.

There is a small anomaly in Fig. 5 because we have frozen the atoms in the core in their initial positions. According to our calculation a 13-atom icosahedron has a lattice dimension of 2.50 Å. However, the core expands to 2.58 Å when the second shell is added to the layer. By freezing the core, we have not allowed these changes in lattice dimension to occur. In order to assess the effects of the changes in the core dimension on the growth sequence, we also calculated an evaporation sequence where we started with a cluster with two or more complete shells and sequentially removed atoms without relaxing the atomic positions. The results were very similar to those in Figs. 3, 4, and 5. The site-filling sequence was identical in the evaporation sequence and in the growth sequence. However, the energies were slightly different. Hence, we have included Fig. 7 a plot of the energies/atom calculated from the evaporation sequence.

III.2. Annealing Sequences

We have also done simulated annealing of the clusters using a Monte Carlo scheme. In a typical annealing sequence we would anneal a cluster at 300–500 K, and then use a conjugate gradient energy minimization technique to quench the clusters to 0 K. The results of these calculations showed that none of the polyhedra clusters are stable, upon annealing to 300 K. If we allow all of the atoms to move, the nonmagic-number clusters will spontaneously reconstruct at 0 K. The magic-number (i.e., filled-shell) clusters are stable at 0 K. However, they spontaneously reconstruct into lower energy structures upon annealing at 300 K. So far we have only done extensive calculations with clusters of 60 atoms or less. However, our initial work with larger clusters indicates that even the 147-atom icosahedron reconstructs to a structure with a 1-eV lower energy upon annealing to 500 K.

In order to try to find clusters which were stable upon annealing, we did a series of calculations where we repetitively annealed the clusters at 500 K, quenched to 0 K, and

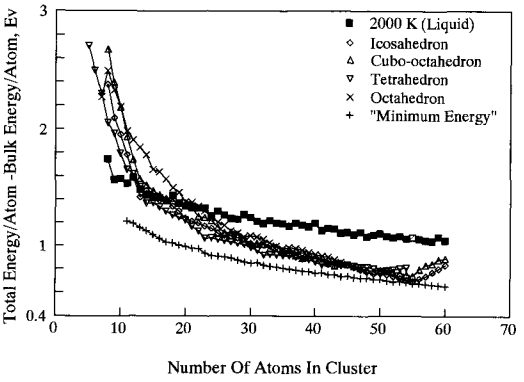

FIG. 7. The energy per atom minus the bulk energy per atom for the evaporation of atoms from (◇) truncated icosahedra, (△) truncated cubo-octahedra, (▽) truncated tetrahedra, (×) truncated octahedra, (■) platinum clusters at 2000 K, and (+) the "minimum energy" clusters.

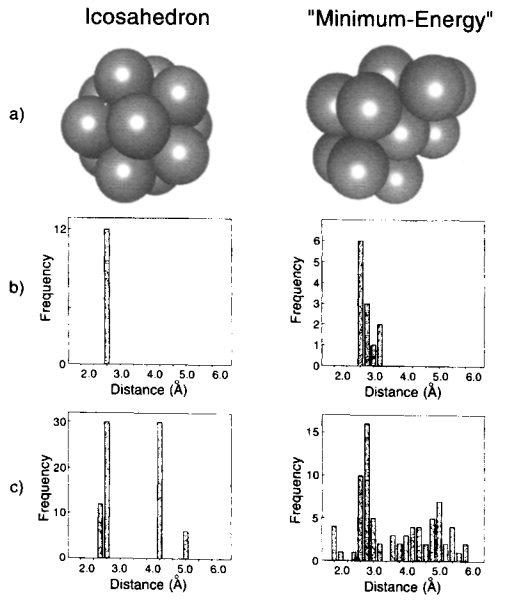

FIG. 8. A comparison of the properties of the 13-atom icosahedron to the properties of the minimum energy 13-atom structure: (a) diagrams of the clusters, (b) the distance between the outer shell atoms and the central atom, (c) the distribution of interatomic distances in the clusters.

looked for clusters with especially low energies. Generally, we annealed for 2000 MC steps, with an acceptance probability of 0.5–0.6, and then quenched using a conjugate gradient scheme. This procedure was repeated for a total of 2,000,000 MC steps and we saved the minimum value structures from all of the runs. It is generally accepted that it is all but impossible to prove that the clusters found in this way do represent the energetically absolute minimum structure. However, care was taken to ensure that the final "minimum-energy" structure was not dependent upon either the number of total iteration steps or the configuration of the starting cluster.

Figures 8 and 9 show some of the minimized cluster shapes we have found, while Table 1 lists the energies of the 13- and 55-atom icosahedra, cubo-octahedra, and the "minimum-energy" clusters. The 13-atom cluster rearranges to a very asymmetric shape upon annealing. This central atom in the 13-atom minimum-energy cluster does not have what could be characterized as nearest neighbors, but instead has neighbors with distances ranging from 2.55 to 3.12 Å as illustrated in Fig. 8. By comparison, the interatomic distances from the central atom to the surface positions in a relaxed icosahedron were all 2.50 Å. As the clusters get larger they assume the spherical shapes shown in Fig. 9. Note that these structures are much more compact than the truncated polyhedra, at the same sizes, which partially explains their stability.

The minimum-energy clusters of sizes lying between the magic numbers are similar to all of the others in the series in that their radial distribution histograms a compilation of all the interatomic distances in the cluster display a more gradual spread in the interatomic separations as shown in Fig. 10. There are however, two different regions of maxima in these histograms, one located in the 2.4–2.8 Å range and the other in the 4–5 Å range. This feature is reminiscent of the shell-like make up of the icosahedral cluster. Another noteworthy attribute of these minimum energy clusters is the absence of any fivefold coordinated surface sites such as those found on the vertex of a icosahedron. In its place is the formation of the sixfold coordinated surface sites.

There is one other feature in the calculations, which was that at the smallest sizes, several different cluster shapes all had similar energies. Bigot and Minot (*27*) also found that in Hückel calculations small platinum

TABLE 1

Energies of the 13- and 55-Atom Icosahedron, Cubo-Octahedron, and Minimum-Energy Cluster

	Energy (eV)	
Cluster	13-Atom	55-Atom
Icosahedron	−57.705	−272.807
Cubo-Octahedron	−56.704	−270.163
Minimum-Energy	−58.431	−273.764

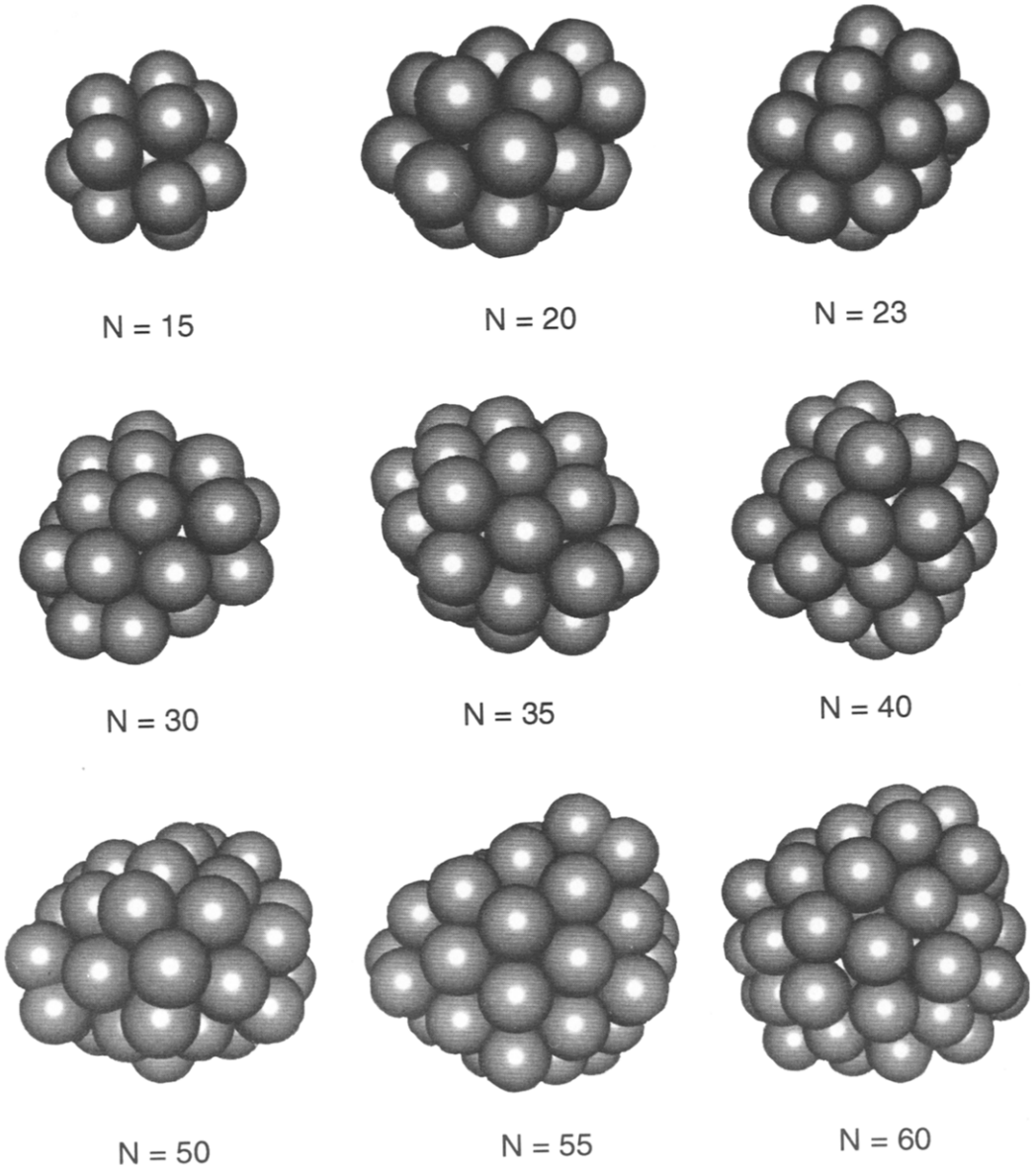

FIG. 9. The structure of the minimum-energy clusters with 15, 20, 23, 30, 35, 40, 50, 55, and 60 atoms.

clusters many different cluster shapes show similar energies. For example, Fig. 11 shows a series of 13-atom clusters which all have an energy within 0.4 eV of the minimum-energy cluster. All of the clusters have an energy at least 0.5 eV below that of a 13-atom icosahedron. Notice that the geometries are different. None of the clusters displays any apparent symmetry. In contrast, the corresponding 13-atom icosahedron is very symmetric. At this point, we cannot characterize these geometries. However, our general finding is that there are many defect structures with very similar energies.

The implication of this result is that there is no single equilibrium shape of clean plati-

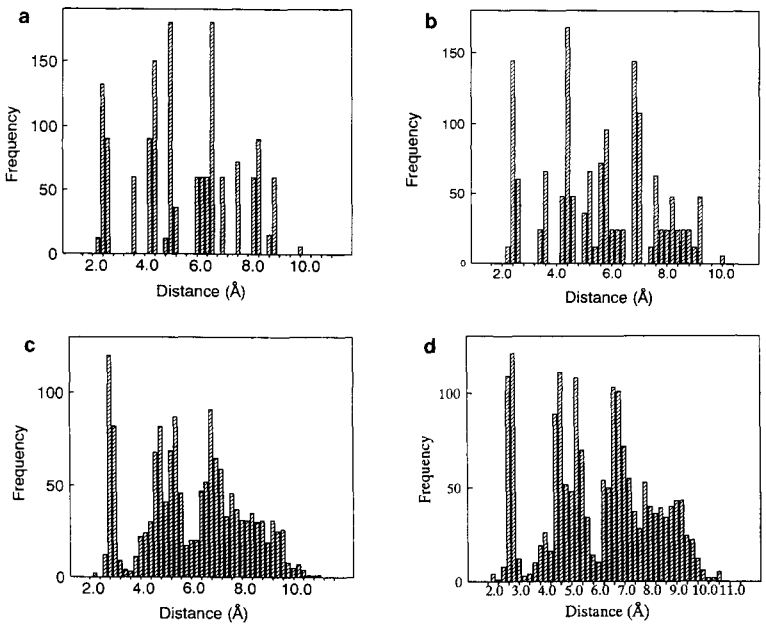

FIG. 10. A comparison of the distribution of atom-atom distances in the (a) 55-atom icosahedron, (b) 55-atom cubo-octahedron, (c) minimum-energy 55-atom cluster, and (d) minimum-energy 60-atom cluster.

num in this size range. Rather, at any finite temperature there should be a wide distribution of cluster shapes in any given sample.

IV. DISCUSSION

Of course, experimentally there is already ample evidence for such a conclusion. For example, in TEM, small supported platinum particles usually show irregular shapes with many defects (*12–14*). People often observe "icosahedral" particles with many defects and twins. However, so far no one has reported seeing a defect-free icosahedral platinum particle.

Our calculations predict that highly defected structures should predominate at smaller particle sizes. The magic-number icosahedra do show some stability. However, defected structures are predicted to be even more stable, in agreement with experiment.

Recently, other calculations to determine the shape and electronic structure of elemental clusters have called into question the notion that the icosahedron is the most sta-

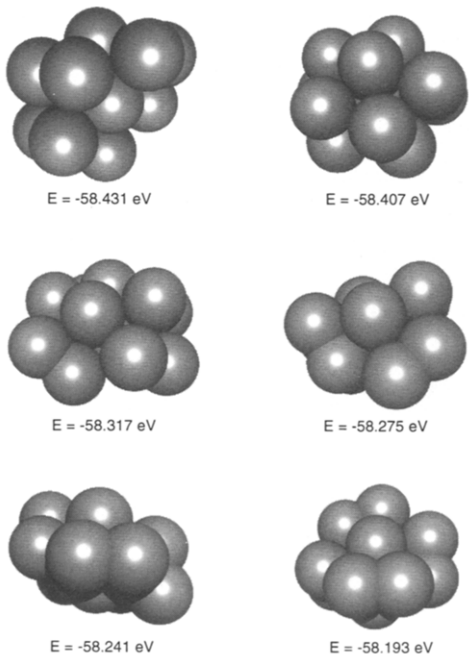

FIG. 11. A series of 13-atom clusters with similar energies but far different geometries.

TABLE 2

The Energies of the Individual Atoms in the 13-Atom Icosahedron and the Minimum-Energy 13-Atom Cluster

Atom No.	13-Atom icosahedron			13-Atom "minimum-energy"		
	Embedding energy (eV)	Core repulsions (eV)	Total energy (eV)	Embedding energy (eV)	Core repulsions (eV)	Total energy E(eV)
1 (Center)	−13.88	10.074	−3.811	−10.26	4.861	−5.402
2	−8.272	3.781	−4.491	−10.73	6.488	−4.237
3	−8.272	3.781	−4.491	−10.91	6.498	−4.415
4	−8.272	3.781	−4.491	−10.59	6.225	−4.366
5	−8.272	3.781	−4.491	−8.58	3.919	−4.660
6	−8.272	3.781	−4.491	−10.98	6.653	−4.330
7	−8.272	3.781	−4.491	−10.80	6.413	−4.391
8	−8.272	3.781	−4.491	−10.55	6.196	−4.359
9	−8.272	3.781	−4.491	−10.84	6.404	−4.438
10	−8.272	3.781	−4.491	−10.93	6.509	−4.420
11	−8.272	3.781	−4.491	−10.60	6.226	−4.377
12	−8.272	3.781	−4.491	−8.91	4.234	−4.673
13	−8.272	3.781	−4.491	−10.37	6.007	−4.364

ble configuration for a 13-atom system. By using a density functional molecular dynamics approach in conjunction with dynamical simulated annealing, Kumar and Car (*28*) have ascertained the optimum shape of a 13-atom magnesium cluster as a fusion of a 4-atom polytetrahedral and a 9-atom trigonal prism cluster. This geometry was found to be 0.043 eV/atom and 0.032 eV/atom lower in energy than an icosahedron and a cubo-octahedron respectively. Investigations (*29*) using the same calculation methods for silicon clusters showed no similarity between the icosahedron and the 13-atom low-energy dynamically simulated annealed structures. Similarly, Bernholc and co-workers (*32*) have also shown that the 13- and 55-atom aluminum clusters can attain more stable structures than the icosahedron and cubo-octahedron. Not only are their geometries significantly more distorted than the latter two polyhedral symmetries, but several structurally inequivalent but energetically degenerate were found to exist. Ours is the first calculation to show that irregular shapes should be stable for platinum in cluster sizes greater than 12 atoms. However, there is already ample evidence for the stability of irregularly shaped particles from other sources.

Another prediction of the calculations is that we do not expect platinum particles to show sharply varying stability with varying particle size. Previous workers have found that many metals show distinct shell structure, where certain key sizes are unusually stable. However, Kaldor and co-workers (*33*) have found that platinum clusters formed by condensation of platinum in the gas phase show a random size distribution. No size predominates. Our calculations show that the energy of our minimum energy clusters varies smoothly with cluster size. There are no sizes which show enhanced stability in the calculations in agreement with Kaldor's measurements.

In summary then, our calculations suggest that small platinum particles should show disordered structures, and no magic numbers. These results agree with experiment.

IV.1. The Origin of the Highly Defected Structures

It is interesting to consider why the defected structures form. Table 2 compares

the potential energies for the individual atoms in a 13 atom icosahedron to those for the minimum energy cluster. Notice that the main advantage in the energy for the minimum-energy structure is derived from the energy difference at the central atom position (atom no. 1). Atom nos. 5 and 12 also exhibit slight energetic gains and contribute towards the enhanced stability of the minimum energy cluster. However, the remaining atomic positions have higher energy values than the equivalent relaxed icosahedron positions.

This energy difference between the central atom in the two structures comes about in the calculations because of enhanced repulsions at the core of the 13-atom icosahedron. The electron density at the core atomic position of the icosahedron is by far the highest and this in turn corresponds to a large embedding energy. However, the atom also has 12 nearest neighbors which are compressed into the central atom, and thereby impart a significant repulsive force. It happens that the repulsive forces largely counteract the attractive forces which leads to the total contribution of only -3.81 eV at the central atom position. The 12 equivalent surface atoms, though embedded in a weaker electron density, are less burdened with the repulsive electrostatic pair component of the potential due to the presence of fewer nearest neighbors. The resulting energy of an individual surface atom, -4.49 eV, is actually lower than the core atom.

In contrast, with the "minimum-energy" 13-atom cluster, the electron densities fall within the density limits of the icosahedral atoms, i.e., 0.022–0.054 $Å^{-3}$. A more even distribution such as this is a result of the seemingly arbitrary arrangement of the atoms in the cluster and follows a similar trend in the interatomic separations observed in the radial distribution histograms. The energetic gain over the icosahedron is made at the central atom which has only nine neighbors with interatomic distances of 3 Å or less. Compare this value with the central icosahedral atom which has 12 neighbors with a lattice parameter of 2.50 Å. So, although the electron density and the resulting embedding energy of the central atom in the "minimum-energy" cluster are lower, the decreased repulsive interactions result in a more favorable energetic outcome for the overall cluster. The advantage gained at this position is sufficient to offset the losses absorbed at most of the remaining surface positions.

It is not immediately obvious why the central atom has so much higher of an energy in the icosahedron than in the minimum-energy cluster. However, we believe that the difference is associated with the way which surface tension compresses the 13-atom cluster. If we start with a 13-atom cluster, and freeze the atoms in their bulk position, we find that the energy of the central atom increases continuously as we remove atoms from the cluster as illustrated in Fig. 12. However, our calculations indicate that with a minimized 13-atom cluster, the platinum atoms are only 2.5 Å apart. This compares to 2.77 Å in the bulk. The compression is interesting in that the atoms are so tightly packed that when we remove one atom, the energy of the core atom goes up! (See Fig. 12.) The energy of the central atom attains the most energetically favorable state when it is surrounded by only eight surface atoms. The inclusion of the remaining four atoms to complete the first shell of the icosahedron results in an increase in the energy of the central atom. This outcome has implications in the determination of optimum coordination numbers of an atom in a cluster. According to the calculations it is best to have a maximum of eight nearest neighbors within an icosahedral framework when the lattice dimension is compressed to 2.5 Å. Any further increase in the number of nearest neighbors causes the cluster to be less energetically stable.

Physically, when the lattice is compressed, the overlap between the bonding electrons in the various atoms increases. One gets as much bonding with 8 nearest neighbors in the compressed lattice as one gets with 12 nearest neighbors in bulk plati-

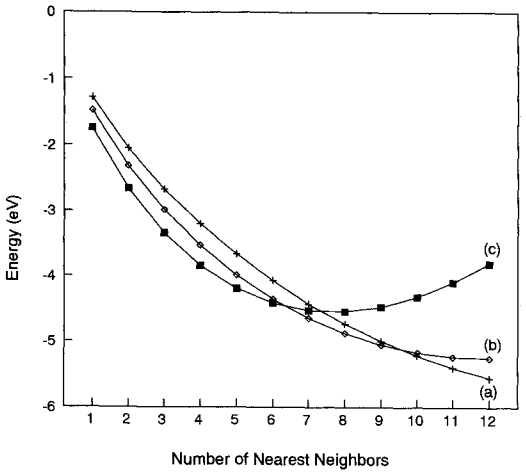

FIG. 12. The energy of the central atom in a truncated-icosahedron as a function of the number of atoms which are adjacent to the central atom calculated at (a) the bulk lattice dimension 2.77 Å, (b) the lattice dimension for a 55-atom cluster, 2.56 Å, and (c) the lattice dimension for a 13-atom icosahedron 2.50 Å.

num. There is still some additional overlap when the 9, 10, 11, and 12 nearest neighbor atoms are added to the cluster which produces a higher embedding energy (i.e., slightly more bonding). Also, the nonlinearity or curvature in the embedding function for platinum is such that there is insufficient extra bonding to sustain the additional repulsive forces brought upon by squeezing four additional neighbors around the central atom. As a result, when the 13-atom cluster is compressed by surface tension, the central atom would only like to have 8 nearest neighbors rather than the 12 nearest neighbors in the bulk. This causes the 13-atom icosahedron to reconstruct.

The 55-atom cluster shows different behavior, however. Like the 13-atom icosahedron, in the two-layer 55-atom icosahedron the central atom possesses the highest electron density and also the lowest embedding energy, but unlike the 13-atom cluster this central atom also has the most favorable total energy. Physically, the lattice compression is smaller with a 55-atom cluster so the central atom is still stable. However, the atoms at the verticies in the surface of the icosahedron are very unstable. The atoms at the vertices of the icosahedron only have five nearest neighbors. They have a low embedding energy which implies that they have little bonding. It works out to be energetically favorable to eliminate the vertex positions, by distorting the rest of the cluster. There are no vertex positions in the 55-atom "minimum-energy" cluster. Instead, the electron densities are now more evenly distributed and like in the 13-atom case, well within the boundaries set forth by the upper and lower limits of the 55-atom icosahedron. We believe that it is the instability of the low coordination vertex sites which causes the 55-atom icosahedron to reconstruct.

We have also observed reconstructions with a 147-atom icosohedral cluster. The vertices round out, and the energy of the cluster decreases by about 1 eV. So far our calculations for the 147-atom cluster are incomplete and so it is unclear whether we have found the minimum-energy shape for a 147-atom cluster. However, the calculations so far show that even a 147-atom icosohedron is unstable to defect formation.

The observations on the structure and shape of these minimum-energy clusters should enable us to say a few words about the factors influencing the stability of small metal clusters. Compactness of the cluster it is believed (*30*) is partly an indicator of enhanced stability as it leads to an increase in the effective coordination number of the cluster. This postulation was supported by the extended Hückel calculations (*27*) on $Pt_n(n = 2–13)$ clusters, which showed that the optimum cohesive energy of the cluster is achieved when the cluster is more spherical and compact.

The main force acting upon the surface of the cluster is the surface tension, which is sometimes referred to as the strain energy. Surface tension has the tendency to pull the atomic cores on the surface closer to the center. This compresses the atoms, and so it costs energy to fill up the inner shell. In the case of the 13-atom platinum cluster the compression causes the optimum number of nearest neighbors to change from 12 in the

bulk to 8 in a small cluster. It is the trade-off between the surface tension and repulsions caused by a lattice compression which determines the final shape of the cluster. In larger clusters the effects of the surface tension are distributed over a much larger surface area thereby reducing the number of defect structures on the surface.

Still multiple twin and stacking faults are seen even in moderate sized platinum particles (*11*). Previous investigators have hypothesized that shapes to the interactions between the surface twin-boundary and elastic strain energies in a particle (*13, 31*). Our results give strong theoretical support to these previous hypotheses, and show quantitatively how the strain (i.e., surface tension) changes the particle shapes.

V. IMPLICATIONS AND SPECULATION

In summary then, the results in this paper show metal particles in catalysts are probably not going to show the cubo-octahedral or icosahedral structures predicted by Hoare (for argon). Rather other less regular shapes should predominate. We find that defected structures have a lower energy than any of the regular polyhedra at sizes up to 60 atoms. We are now doing calculations for larger sized clusters, and have found that even the 147-atom icosahedron reconstructs to a lower energy structure upon annealing at 500 K. There is a need to verify these results with some other calculational technique. However, our results suggest that in contrast to what it says in most textbooks one should not expect to observe perfect icosahedrons or cubo-octahedrons in supported platinum catalysts.

Of course, the calculations described above apply only to isolated unsupported platinum clusters. Hence, some care has to be taken before extrapolating these results to real supported catalysts. It can be expected that once the support effects are incorporated in these simulations that some changes would be observed in the structures of the stable cluster geometries. It was found that a number of cluster geometries could exist for a given size with only minimal differences in total energy. These energetic isomers are commonly observed in clusters prepared in the gas phase as is evidenced by the wide distribution of the mass spectrum. Therefore only a slight contribution due to a support effect could conceivably result in a different "minimum-energy" cluster geometry. It is quite possible our minimum-energy cluster may not be the minimum-energy cluster in a supported platinum catalyst.

However, we can say that it is very likely that the most stable platinum cluster is going to be high defected. In our calculations, the defected structures were 1–2 eV below the icosahedrons. It is difficult to imagine how the energy of an icosahedron could be lowered enough to stabilize the icosahedron in the presence of the support. Certainly, perfect icosahedrons are not seen experimentally.

It is also very likely that the smallest particles in supported platinum will show surface structures which are unstable in bulk platinum. Our clusters are very asymmetric. There are surface structures in our calculations which do not exist in bulk platinum. Our particle shapes seem to have some correspondence to the ones seen experimentally.Therefore, there is reason to suspect that one might also observe highly defected surface structures in supported platinum catalysts if one could find a way to measure the surface structure.

At this point, we do not even have the nomenclature needed to describe the surface structure of our clusters, and so we cannot really describe the types of surface sites available for reaction. However, it is clear that the old ideas about what surface structures of supported particles are like do not apply to our particles. Hence, there is a need to rethink what particles are like in catalysts based on our findings.

ACKNOWLEDGMENTS

This work was supported by the National Science Foundation under Grant DMR 89-20358. The authors thank Murray Daw, Steve Foiles, and Mike Baskes for

providing a copy of the EAM code, a modified version of which was used for all of the calculations in this paper.

REFERENCES

1. Hoare, M. R., and Pal, P., *Adv. Chem. Phys.* **20,** 161 (1971).
2. Hoare, M. R., and Pal, P., *Adv. Chem. Phys.* **24,** 645 (1975).
3. Hoare, M. R., and McInnes, J., *Adv. Phys.* **32,** 791 (1983).
4. Hoare, M. R., and Pal, P., *J. Cryst. Growth* **17,** 77 (1972).
5. Farges, J., de Feraudy, M. F., Raoult, B., and Torchet, G., *J. Chem. Phys.* **78,** 5067 (1983).
6. Raoult, B., Farges, J., de Feraudy, M. F., and Torchet, G., *Philos. Mag. B* **60,** 881 (1989).
7. van der Waal, B. W., *J. Chem. Phys.* **90,** 3407 (1989).
8. Burton, J. J., *Catal. Rev.-Sci. Eng.* **9,** 209 (1974).
9. Lee, J. W., and Stein, G. D., *J. Phys. Chem.* **91,** 2450 (1987).
10. Briant, C. L., and Burton, J. J., *J. Chem. Phys.* **63,** 2045 (1975).
11. Yacaman, M. J., Heinemann, K., Yang, C. Y., and Poppa, H., *J. Cryst. Growth* **47,** 187 (1979).
12. Marks, L. D., and Smith, D.J., *J. Cryst. Growth* **54,** 425 (1981).
13. Howie, A., and Marks, L.D., *Philos. Mag. A* **49,** 95 (1984).
14. Marks, L. D., *J. Cryst. Growth* **61,** 556 (1983).
15. Lee, W. H., Vanloon, K. R., Petrova, V., Woodhouse, J. B., Loxton, C.M., and Masel, R.I., *J. Catal.* **126,** 658 (1990).
16. Daw, M. S., and Baskes, M. I., *Phys. Rev. B* **29,** 6443 (1984).
17. Schwoebel, P. R., Foiles, S. M., Bisson, C. L., and Kellog, G. L., *Phys. Rev. B* **40,** 10639 (1989).
18. Wright, A. F., Daw, M. S., and Fong, C. Y., *Phys. Rev. B* **42,** 9409 (1990).
19. Foiles, S. M., *Surf. Sci.* **191,** L779 (1987).
20. Daw, M. S., *Surf. Sci.* **166,** L161 (1986).
21. Chen, S. P., and Voter, A. F., *Surf. Sci.* **244,** L107 (1991).
22. Hsieh, H., and Averback, R. S., *in* "Proceedings of the Materials Research Society Symposium," Vol. 206, Materials Research Society, Pittsburgh, PA, 1991.
23. Cleveland, C. L., and Landman, U., *J. Chem. Phys.* **94,** 7376 (1991).
24. Sinclair, J. E., and Fletcher, R., *J. Phys. C.* **7,** 864 (1974).
25. Foiles, S. M., Baskes, M. I., and Daw, M. S., *Phys. Rev. B* **33,** 7983 (1986).
26. Allpress, J. G., and Sanders, J. V., *Aust. J. Phys.* **23,** 23 (1970).
27. Bigot, B., and Minot, C., *J. Am. Chem. Soc.* **106,** 6601 (1984).
28. Kumar, V., and Car, R., *Z. Phys. D* **19,** 177 (1991).
29. Andreoni, W., *Z. Phys. D.* **19,** 31 (1991).
30. Koutecky, J., and Fantucci, P., *Z. Phys. D* **3,** 147 (1986).
31. Marks, L. D., *Philos. Mag. A* **49,** 81 (1984).
32. Yi, J.-Y.,Oh, D. J., and Bernholc, J., *Phys. Rev. Lett.* **67,** 1594 (1991).
33. Whetten, R. L., Cox, D. M., Trevor, D. J., and Kaldor, A., *Surf. Sci.* **156,** 8 (1985). Kaldor, A., Cox, D. M., *Pure Appl. Chem.* **62,** 79 (1990), and references therein.
34. Martin, T. P., Bergman, T., Göhlich, H., Lange, T., *J. Phys. Chem.* **95,** 6421 (1991).